

## AN INVESTIGATION OF THE INFLUENCE OF THE SUSPENSION CONSTRUCTION PARAMETERS ON THE PERFORMANCES OF THE RAILWAY VEHICLES

Ioan SEBEȘAN<sup>1</sup>, Dan BĂIAȘU<sup>2</sup>, Gheorghe GHIȚĂ<sup>3</sup>

<sup>1</sup>“Politehnica” University Bucharest, Faculty of Transports, Bucharest, Romania

<sup>2</sup> Atelierele CFR Grivita S.A., Calea Grivitei 359, 010178, Bucharest, Romania

<sup>3</sup>Romanian Academy, Institute of Solids Mechanics – IMSAR, Bucharest, Romania

E-mail: gh\_ghita@yahoo.com

The paper aims to present a study of the construction parameter influence of a railway vehicle suspension on its performances: safety and comfort. To simulate the lateral dynamics of the vehicle is used a multibody model with 17 degrees of freedom. This model considers the lateral, yawing and rolling oscillations, the geometrical nonlinearities of the wheel-track contact and assesses the nonlinear stability of the vehicle running on tangent tracks with irregularities. To reduce the lateral accelerations generated by the track irregularities, the authors introduced in the secondary suspension of the vehicle a device with sequential damping based on balance-logic control strategy and shown that the use of a semi-active suspension improves the safety and the comfort of the railway vehicle. The system response in terms of accelerations is compared for both passive and semi-active cases.

*Key words:* railway vehicle, specific non-linear phenomenon, multibody method, non-linear mathematical model, semi-active damper, balance logic control.

### 1. INTRODUCTION

High-speed trains are increasingly present in the landscape of contemporary means of transport, being efficient, economic and environmental friendly. The rails with geometric irregularities, to high speeds, generate large amplitude oscillations of the axles, bogies and carbody. These rail irregularities, above a specific speed value – the critical speed – leads to unstable movement of the vehicle. The frequency of the random excitation from the rail and the vehicle speed [12, 13] determine the dynamic response of the vehicle running on rails with geometric irregularities. In the present paper, a mathematical model, which simulates the lateral dynamics of the carbody, has been integrated. Using the instrument it is carried on a study of vehicle stability, taking into consideration both linear and nonlinear aspects. It is highlighted the influence of the construction parameters of the suspension systems upon the vehicle behavior at high speeds.

In the article, the authors demonstrate that there are opportunities to increase vehicle performance through proper design of the vehicle suspension.

### 2. THE MATHEMATICAL MODEL OF THE VEHICLE

#### 2.1. Simplifying hypotheses of the model

The mathematical model used in this article was determined considering all the elastic and damping elements forming the classical suspension systems are weightless and have linear characteristics. Under conditions of geometrical, elastic and inertial symmetry, with identical wheel and rail patterns, the equilibrium position of the carbody coincides with its median position in relation to the tracks. The rolling surface contact angles are small and the radii of curvature for the rolling treads remain unchanged. Conicity has been considered as having an equal constant value with the rolling surface effective conicity. The geometrical and elastic symmetry of the mechanical model facilitates the decoupling of the lateral

movements from the vertical ones [1, 8 ÷ 10]. To study the vehicle lateral oscillations, the mechanical model considers the following degrees of freedom:  $y_c, \psi_c, \varphi_c, y_{bj}, \psi_{bj}, \varphi_{bj}, y_i, \psi_i$ , where  $j = 1, 2$  represent the bogies and  $i = 1 \div 4$  – the wheelsets.

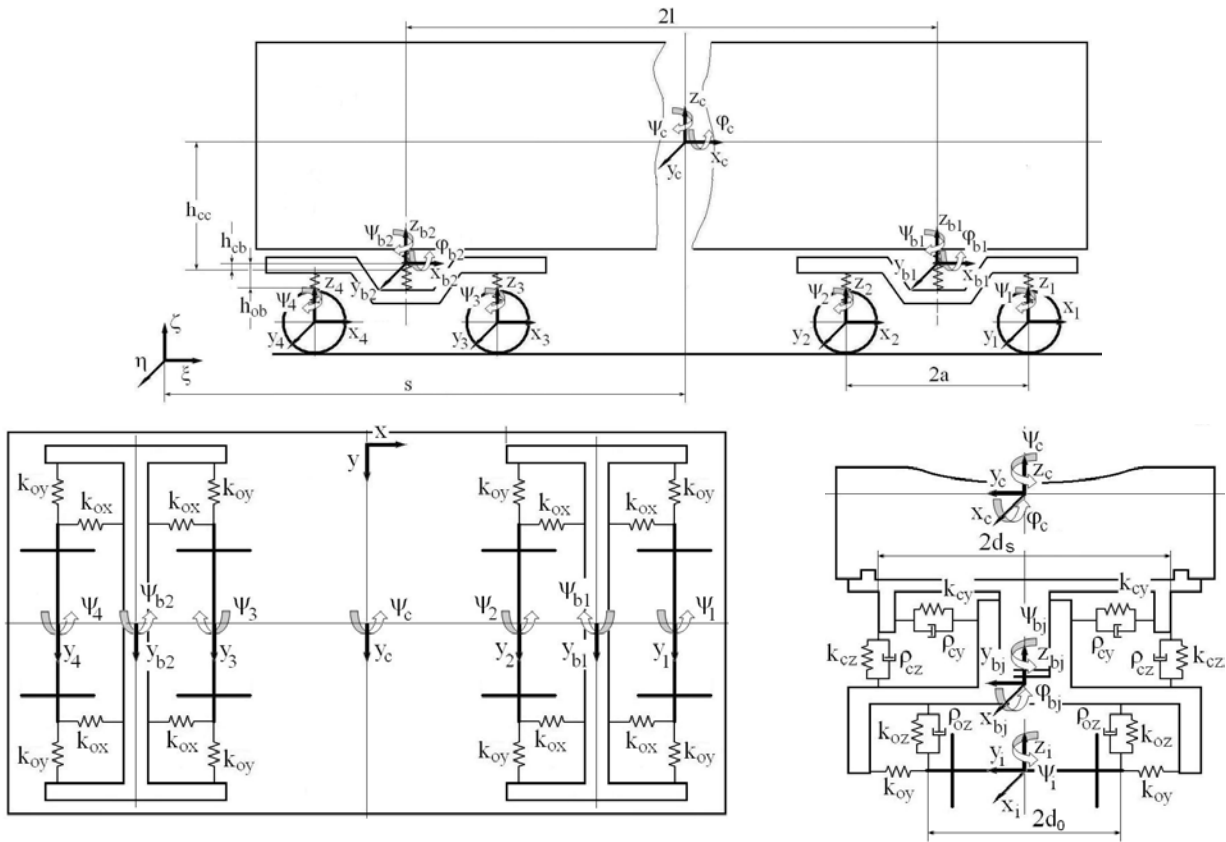


Fig. 1 – The railway vehicle model.

**2.2. The wheel – track contact forces**

In accordance with the Kalker’s linear theory [6] the contact forces are:

$$F'_x = -f_{33}\xi_x, \quad F'_y = -f_{33}\xi_y - f_{12}\xi_{sp}, \quad M'_z = f_{12}\xi_y - f_{22}\xi_{sp}, \quad (1)$$

where:  $F'_x$  - longitudinal creep force,  $F'_y$  - lateral creep force and  $M'_z$  - spin creep moment,  $\xi_x, \xi_y, \xi_z$  - longitudinal, lateral and spin creepages and  $f_{12}, f_{22}, f_{33}$  - creep coefficients.

The resultant creep force cannot exceed the adhesion force. The nonlinear effect of the adhesion limit is considered by computing:  $\sqrt{F'^2_x + F'^2_y} \leq \mu Q$ , where,  $\mu$  - Coulomb friction coefficient,  $Q$  - wheel normal load. For the case that does not consider the spin creepage the limiting resulting force was calculated using the saturation coefficient according to Vermeulen – Johnson’s nonlinear theory presented in [6].

**2.3. The rail inputs**

The railway vehicles operate in a wide diversity of conditions not allowing building an overall mathematical model, which considers all the rail-vehicle interactions. Several representations of the track geometry were included in the dynamic models of the railway vehicles presented in the literature, [2, 5, 8, 13], as dynamic input of the system. In the present paper, the tangent track irregularities are considered periodical, expressed with a sinusoid type expression, according to [8]:

$$\eta_{1,2} = \eta_0 \cos[2\pi(vt + l \pm a) / L], \quad \eta_{3,4} = \eta_0 \cos[2\pi(vt - l \pm a) / L]. \quad (2)$$

The expressions (2) in which  $\eta_0$  is the nominal amplitude of the periodic irregularities depending on the track category,  $L$  – the wavelength of the irregularities,  $l$  and  $a$  – constructive data of the vehicle presented in Table 1,  $v$  – the speed (consider the distance between the axles of the vehicle).

To describe an isolate variation of the track geometry type bump (a single period sinusoid function) and provide the variation of its dimensions according to the vehicle speed, function (3) was used:

$$f(\Delta) = \frac{1 - \cos \left[ 2\pi v \left( t - \frac{s_0}{v} \right) \right]}{\Delta} v, \tag{3}$$

where  $\Delta$  is the length of the irregularity and  $s_0$  – the distance to the track deformation.

The function (4)  $h v_i$  describes delay of the contact between the track bump (single deformation) and the vehicle axles:

$$h v_i = f(\Delta) \cdot \left[ H \left( t - \frac{s_i}{v} \right) - H \left( t - \frac{s_i + \Delta}{v} \right) \right], \tag{4}$$

where  $H(x)$  is the generalized Heaviside’s function. The parameter  $s_i$  describing the position of each axle will simulate the delay of the contact axle-rail irregularity.

### 2.4. The lateral dynamics equations

The vehicle is considered as it is composed of a limited number of rigid bodies, simulating its main parts, connected in between through mechanical weightless linkages: the carbody, the bogies and the wheelsets [11, 12]. To position each of the rigid bodies forming the model of the vehicle will be used an inertial reference frames coordinate system whose origin is fixed in space and time.

The constraint conditions are expressed as nonlinear algebraic equations, depending on the generalized coordinates and time.

The  $O_c \xi \eta \zeta$  is an inertial reference frame originating in the wheelset plan, on the track axis, at a distance  $s$  from the  $O_c$  carbody center of mass (Fig. 1). The relative displacements of the multibody model elements it will be determined by as the difference between the position vectors of the suspension center with respect to the rigid bodies representing each suspension level.

The vectors of the relative displacements between the carbody and the bogies and the vectors of the relative displacement between the bogies and the axles are:

$$x_c - x_{b_j} = -(-1)^j a, \quad z_c - z_{b_j} = h_{cc} + h_{cb},$$

$$r^c - r^{b_j} = \begin{bmatrix} -(\psi_c - \psi_{b_j})(\pm d_s) \\ y_c + h_{cc} \phi_c + (-1)^{j+1} l \psi_c - y_{b_j} + h_{cb} \phi_{b_j} \\ (\phi_c - \phi_{b_j})(\pm d_s) \end{bmatrix}, \quad r^{b_j} - r^i = \begin{bmatrix} -(\psi_{b_j} - \psi_i)(\pm d_o) \\ y_{b_j} + (-1)^{i+1} a (\psi_{b_j} - \psi_i) + h_{ob} \phi_{b_j} - y_i \\ (\pm d_o) \phi_{b_j} \end{bmatrix}. \tag{5}$$

The oscillating kinetic energy of the system, potential energy and the energy dissipation function has the expressions presented in (6) where:  $E$  – kinetic energy;  $V$  – potential energy and  $D$  – dissipated energy. In (6) upper indexes represent the direction of motion and lower indexes represent:  $c$  – carbody;  $b_j$  – bogies;  $o_i$  – wheelsets.

The equations of the generalized forces (7), that are considered refers to  $y_i$  and  $\psi_i$  degrees of freedom of the wheelsets, are established using the wheelset efforts diagram presented in [4] and (Fig. 2).

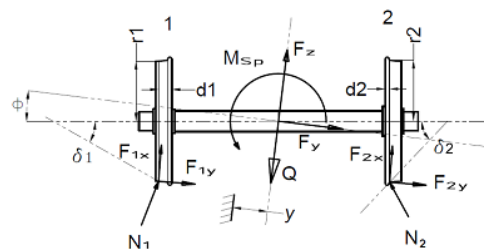


Fig. 2 – The wheelsets efforts diagram

$$\begin{aligned}
E &= E_{y_c} + E_{\psi_c} + \sum_{j=1}^2 E_{y_{bj}} + \sum_{j=1}^2 E_{\psi_{bj}} + \sum_{j=1}^2 E_{\varphi_{bj}} + \sum_{i=1}^4 E_{y_i} + \sum_{i=1}^4 E_{\psi_i} \\
V &= \sum_{j=1}^2 V_{cb_j}^y + \sum_{j=1}^2 V_{cb_j}^x + \sum_{j=1}^2 V_{cb_j}^z + \sum_{i=1}^2 V_{b_1o_i}^y + \sum_{i=3}^4 V_{b_2o_i}^y + \sum_{i=1}^2 V_{b_1o_i}^x + \sum_{i=3}^4 V_{b_2o_i}^x + \sum_{i=1}^2 V_{b_1o_i}^z + \sum_{i=3}^4 V_{b_2o_i}^z \\
D &= \sum_{j=1}^2 D_{cb_j}^y + \sum_{j=1}^2 D_{cb_j}^x + \sum_{j=1}^2 D_{cb_j}^z + 2 \sum_{j=1}^2 D_{b_jo}^z.
\end{aligned} \tag{6}$$

The generalized forces are  $Q_{y_i}$  (generated by the lateral forces) and  $Q_{\psi_i}$  (due to the yaw moments acting on the wheelsets):

$$\begin{aligned}
Q_{y_i} &= (F_{1y} + F_{2y} + N_1 \sin(\delta_1 - \varphi) - N_2 \sin(\delta_2 + \varphi) + F_g + F_c)_i, \\
Q_{\psi_i} &= \left[ (R_{1x} F_{1y} - R_{1y} F_{1x}) + (R_{2x} F_{2y} - R_{2y} F_{2x}) + R_{1x} N_1 \sin(\delta_1 - \varphi) - \right. \\
&\quad \left. - R_{2x} N_2 \sin(\delta_2 + \varphi) + M_1 + M_2 + M_{sp} \right]_i,
\end{aligned} \tag{7}$$

where:

– the creep forces and moments, for  $k = 1, 2$  the wheels of an axle:

$$\begin{aligned}
F_{kx} &= -\frac{f_{33}}{v} \left[ v \left( 1 - \frac{r_k}{r_0} \right) + (-1)^{k+1} e \dot{\psi} \right] \cos \psi + \frac{f_{11}}{v} (\dot{y} + r_k \dot{\varphi} - v \psi) \cos(\delta_k - (-1)^{k+1} \varphi) \sin \psi + \\
&\quad + \frac{f_{12}}{v} \left( \dot{\psi} + (-1)^{k+1} \frac{v}{r_0} \delta_k \right) \cos(\delta_k - (-1)^{k+1} \varphi) \sin \psi,
\end{aligned} \tag{8}$$

$$\begin{aligned}
F_{ky} &= -\frac{f_{33}}{v} \left[ v \left( 1 - \frac{r_k}{r_0} \right) + (-1)^{k+1} e \dot{\psi} \right] \sin \psi - \frac{f_{11}}{v} (\dot{y} + r_k \dot{\varphi} - v \psi) \cos(\delta_k - (-1)^{k+1} \varphi) \cos \psi - \\
&\quad - \frac{f_{12}}{v} \left( \dot{\psi} + (-1)^{k+1} \frac{v}{r_0} \delta_k \right) \cos(\delta_k - (-1)^{k+1} \varphi) \cos \psi,
\end{aligned} \tag{9}$$

$$M_k = \frac{f_{12}}{v} (\dot{y} + r_k \dot{\varphi} - v \psi) \cos(\delta_k - (-1)^{k+1} \varphi) - \frac{f_{22}}{v} \left( \dot{\psi} + (-1)^{k+1} \frac{v}{r_0} \delta_k \right) \cos(\delta_k - (-1)^{k+1} \varphi); \tag{10}$$

– the lateral and yaw gravitational stiffness, the normal reactions, the spin moment of the wheelset:

$$F_g = Q \left( \frac{\delta_2 - \delta_1}{2} + \varphi \right), \quad M_g = -e \cdot \psi \cdot Q \frac{\delta_1 + \delta_2}{2}, \tag{11}$$

$$N_1 = \frac{1}{2} Q \cdot t \cdot g(\delta_1 - \varphi), \quad N_2 = -\frac{1}{2} Q \cdot t \cdot g(\delta_2 + \varphi), \quad M_{sp} = I_{oy} \frac{v}{r_0} \dot{\varphi};$$

– the position vectors of the contact points:

$$\begin{aligned}
R_{1x} &= (e + \Delta r_1) \cdot \psi, \quad R_{1y} = -(e + \Delta r_1) \cdot \psi + r_1 \cdot \varphi \\
R_{2x} &= -(e - \Delta r_2) \cdot \psi, \quad R_{2y} = (e - \Delta r_2) \cdot \psi + r_2 \cdot \varphi.
\end{aligned} \tag{12}$$

The simplifying hypotheses are:

$$\left( \frac{r_2 - r_1}{2} \right)_i = \lambda \cdot y_i, \quad \left( \frac{r_2 + r_1}{2} \right)_i = r_0, \quad \left( \frac{\delta_2 - \delta_1}{2} \right)_i = 0, \quad \left( \frac{\delta_2 + \delta_1}{2} \right)_i = \lambda, \quad \varphi_i = \frac{\lambda}{e} y_i. \tag{13}$$

By substituting the relations (8) ÷ (11) in the equations (7) and using (13), they are obtained the simplified expressions of the generalized forces corresponding to the generalized coordinates  $y_i$  and  $\psi_i$ :

$$\begin{aligned}
 Q_{y_i} &= -2 \frac{\varepsilon f_{11}}{v} \left[ \left( 1 + r_0 \frac{\lambda}{e} \right) \dot{y}_i - v \psi_i \right] - \frac{2 \varepsilon f_{12}}{v} \dot{\psi}_i - \frac{Q \lambda}{e} (y_i - \eta_i), \\
 Q_{\psi_i} &= -2 \varepsilon f_{33} e \left[ \frac{\lambda}{r_0} (y_i - \eta_i) + \frac{e}{v} \dot{\psi}_i \right] + 2 \frac{\varepsilon f_{12}}{v} \left[ \left( 1 + r \frac{\lambda}{e} \right) \dot{y}_i - v \psi_i \right] - I_{oy} \frac{v}{r_0} \frac{\lambda}{e} \dot{y}_i - \frac{2 \varepsilon f_{22}}{v} \dot{\psi}_i + e Q \lambda \psi_i,
 \end{aligned}
 \tag{14}$$

where  $\eta_i$  is the track deviations on transversal direction.

Applying Lagrange's equations for the mathematical model of the railway vehicle (model with 17 degrees of freedom) it can be obtained the motion equations for the carbody, bogies and axles.

### 3. THE RAILWAY VEHICLE RESPONSE

The equation representing the mathematical model of the lateral motion of the railway vehicle is:

$$[M] \{\ddot{q}\} + [C] \{\dot{q}\} + [K] \{q\} = \{F(t)\},
 \tag{15}$$

where  $[M]$ ,  $[C]$  and  $[K]$  are the mass, damping and stiffness matrixes of the vehicle system,  $\{q\}$  are the generalized displacements vectors and  $\{F(t)\}$  is the vector of the excitation given by the tracks.

With the variable change  $\{y\} = \begin{Bmatrix} \{q\} \\ \{\dot{q}\} \end{Bmatrix}$  the equation (16) is:

$$\{\dot{y}\} = [E] \{y\} + \{F^*(t)\},
 \tag{16}$$

where 
$$[E] = \begin{bmatrix} [0] & [I] \\ -[M]^{-1}[K] & -[M]^{-1}[C] \end{bmatrix} \quad \{F^*(t)\} = \begin{Bmatrix} \{0\} \\ [M]^{-1} \{F(t)\} \end{Bmatrix}.
 \tag{17}$$

The equations (16) are employed both for the study of the system response and of the stability.

Table 1

Construction data of the vehicle

Carbody mass	$m_c = 30760 \text{ kg}$	The distance between the primary suspension springs	$2d_o = 2 \text{ m}$
Bogie mass	$m_b = 2300 \text{ kg}$	Primary suspension damping suspension	$\rho_{oz} = 3,67 \text{ kN/m/s}$
Wheelset mass	$m_o = 1410 \text{ kg}$	The track's gauge	$2e = 1,435 \text{ m}$
Carbody moments of inertia	$I_{cx} = 53596 \text{ kgm}^2$ $I_{cz} = 1661732 \text{ kgm}^2$	The bogie's wheelbase	$2a = 2,560 \text{ m}$
Bogie moments of inertia	$I_{bx} = 2240 \text{ kgm}^2$ $I_{bz} = 2965 \text{ kgm}^2$	The distance carbody center – secondary suspension	$h_{cc} = 1,24 \text{ m}$
Axles moments of inertia	$I_{oy} = 980 \text{ kgm}^2$ $I_{ox} = 100 \text{ kgm}^2$	The distance primary suspension - bogie center	$h_{ob} = 0,01 \text{ m}$
Secondary suspension stiffness	$k_{cx} = 133 \text{ kN/m}$ $k_{cy} = 133 \text{ kN/m}$ $k_{cz} = 473 \text{ kN/m}$	The distance secondary suspension - bogie center	$h_{cb} = 0,06 \text{ m}$
Primary suspension stiffness	$k_{ox} = 256 \text{ kN/m}$ $k_{oy} = 885 \text{ kN/m}$ $k_{oz} = 904 \text{ kN/m}$	Wheel tread radius	$r_o = 0,460 \text{ m}$
		Load on wheel	$Q = 51250 \text{ N}$
Secondary suspension damping	$\rho_{cx} = 0 \text{ kN/m/s}$ $\rho_{cy} = 25 \text{ kN/m/s}$ $\rho_{cz} = 18 \text{ kN/m/s}$	The creepage coefficient	$\chi = 190$
		The spin creepage coefficient	$\chi_s = 0,83$
The distance between bogies	$2l = 17,2 \text{ m}$	The effective wheel conicity	$\gamma = 0,14$
The distance between the secondary suspension's springs	$2d_s = 2 \text{ m}$	The maximum testing speed	$v_{max} = 50 \text{ m/s}$

To simulate the vehicle response in assumption that it runs on a tangent track with a constant speed we used the construction characteristics presented in Table 1.

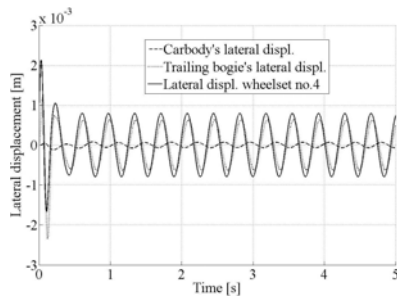


Fig. 3 – The lateral displacement.

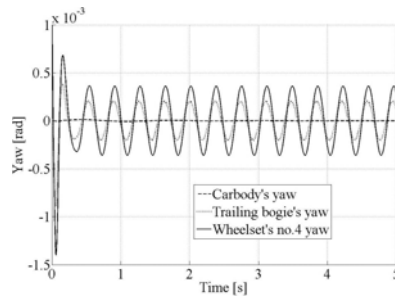


Fig. 4 – The yaw.

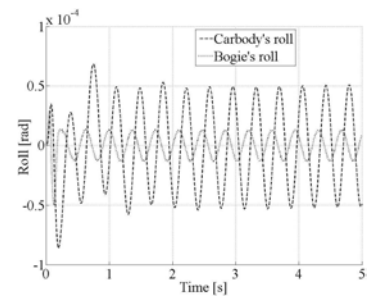


Fig. 5 – The roll.

The diagram study, presented in Figs. 3 ÷ 5, indicates that the main suspension of the carbody acts correspondingly and meets the comfort demands inside the carbody (at the carbody level, the track perturbation effect is reduced compared to the bogie and axles).

#### 4. THE RAILWAY VEHICLE STABILITY

There were simulated two important nonlinearities affecting the wheel-track contact: the nonlinearity of the wheel – track flanging and the creep saturation. If the moving wheelset amplitudes are small, the movement is not influenced by the non-linearities [3, 7].

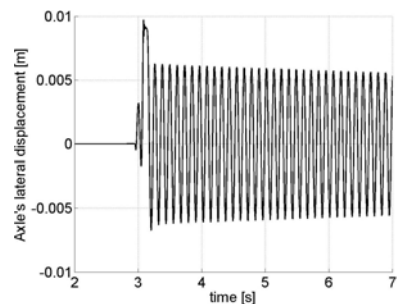


Fig. 6 – Axle lateral displacement,  $v < 245,6$  km/h.

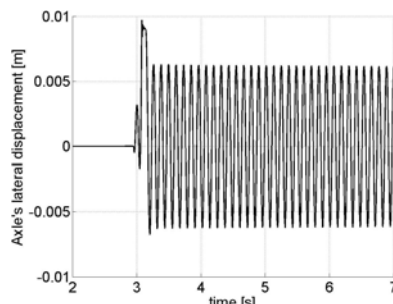


Fig. 7 – Axle lateral displacement,  $v = 245,6$  km/h.

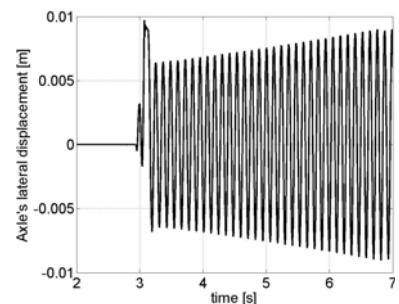


Fig. 8 – Axle lateral displacement,  $v > 245,6$  km/h.

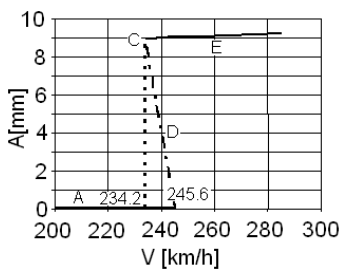


Fig. 9 – Hopf bifurcation diagram of the railway vehicle.

For a vehicle with constructive parameters presented in Table 1, the linear critical speed was determined at a value of  $v = 245.6$  km/h. Figs. 6 ÷ 8 presented the carbody response at inferior, equal and superior speeds to the linear critical speed.

In Fig. 9,  $v = 234.2$  km/h is the nonlinear critical speed and  $v = 245.6$  km/h is the linear critical speed. For any speed under  $v = 234.2$  km/h, the system is asymptotically stable and any perturbation of the vehicle movement along the rail will decrease exponentially. If the speed of the vehicle is between  $v = 234.2$  km/h and  $v = 245.6$  km/h, there are several possibilities for the system movement. For speeds greater than  $v = 245.6$  km/h the solution of the system is unstable. The point of the diagram with the coordinates (245.6; 0) is consequently a bifurcation point.

#### 5. THE INFLUENCE OF THE SUSPENSION PARAMETERS ON VEHICLE STABILITY

In this chapter, the authors will analyze the influences of the suspension parameters (the stiffness and the damping of both suspension levels of the railway vehicle) on vehicle stability and comfort.

### 5.1. The primary suspension stiffness and damping

In the following diagrams – Fig. 10 – it is plotted the influence of the variation of the primary suspension lateral stiffness on the linear and nonlinear critical speed.

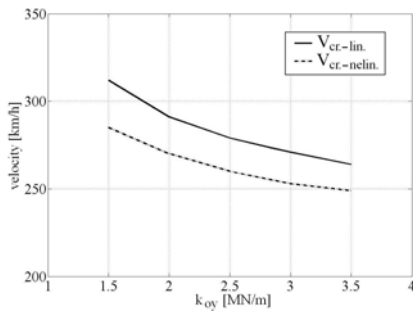


Fig. 10 – Primary suspension lateral stiffness influence on critical speed.

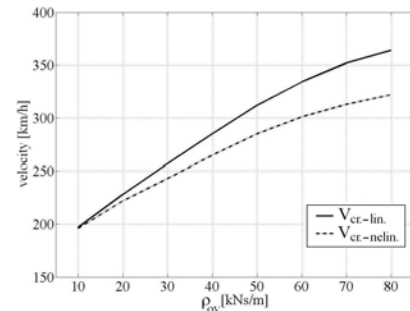


Fig. 11 – Primary suspension lateral damping influence on critical speed.

For greater values of the lateral stiffness,  $k_{oy}$  it appears a very interesting effect of approach between the values of the linear and non-linear critical speeds. In Fig. 11 are plotted the diagrams of linear and non-linear critical speeds against the lateral damping coefficients variation. It is notable the fact that by increasing the damping coefficient  $\rho_{oy}$  has the effect of increasing the value of the critical velocity and the improvement of the vehicle performances in terms of safety are more effective.

### 5.2. The secondary suspension stiffness and damping

The effect of variation of the secondary lateral suspension as presented in Fig. 12 is in the sense of increasing the critical speed. Practically, the secondary suspension damping influences the comfort of the railway vehicle. The variation of the secondary suspension damping does not have an important influence on the wheelsets critical speed (Fig. 13).

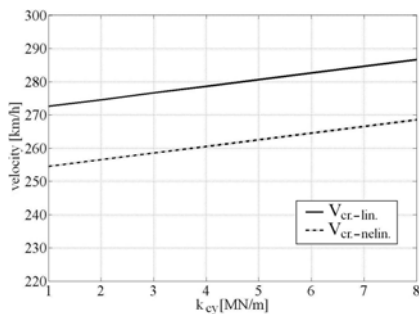


Fig. 12 – Secondary suspension lateral stiffness influence on critical speed.

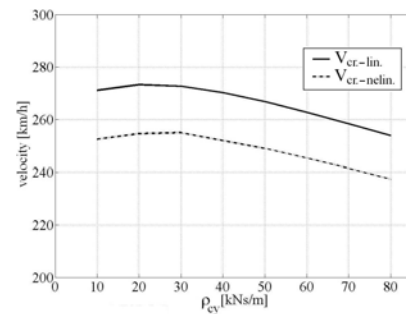


Fig. 13 – Secondary suspension lateral damping influence on critical speed.

According to UIC 518 leaflet, the maximal values of the accelerations should not exceed  $2.5 \text{ m/s}^2$ . The result of using the more rigid dampers in the secondary suspension damage the comfort due to the effect of the coupling between lateral oscillations of the bogie and carbody – Fig. 14. A possibility to go further, to continue to increase the vehicle speed without affecting the comfort is to introduced in the secondary suspension, on the lateral direction, a semi-active damper having a sequential control strategy type balance-logic [11] :

$$\rho_{cy} = \begin{cases} 2\alpha k_{cy} |\Delta y_c| \text{sgn}(\Delta \dot{y}_c), & \Delta y_c \Delta \dot{y}_c < 0 \\ 0, & \Delta y_c \Delta \dot{y}_c > 0 \end{cases} \quad (18)$$

where:  $\alpha$  is a proportion coefficient,  $\Delta y_c$  is the relative lateral displacement in the secondary suspension, and  $\Delta \dot{y}_c$  is the relative lateral speed between the bogie and the carbody. In Fig. 15 is presented the effect of using a semi-active damper with a balance-logic control strategy. This damper reduces the values of the lateral accelerations and improving the railway vehicle comfort.

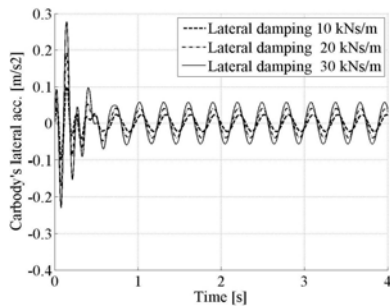


Fig. 14 – The lateral accelerations of the carbody.

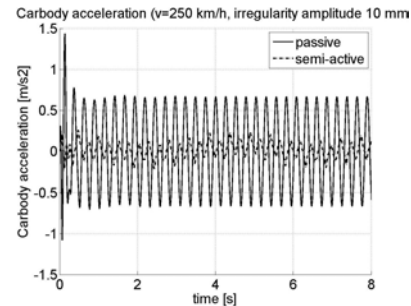


Fig. 15 – The effect of the semi-active suspension.

## 6. CONCLUSIONS

The non-linear mathematical model describing the vehicle movement on a lateral direction was solved through numerical methods in order to determine its component response to the carbody movement on an irregular track. The multibody system based formulation provides a reliable method for the study of the carbody lateral dynamics.

The paper highlights aspects of the non-linear response of the dynamic system to the specific operation conditions and using simulation computer techniques determines the critical speed through non-linear and linear approaches and the response of the carbody.

A parametric study of the influence of the suspension construction on the vehicle performances by means of the non-linear and linear critical speed is carried on.

It is proven that constructive parameters as the suspensions stiffness can considerably improve vehicle safety. In the same time, the possibilities to improve the performances of the vehicle equipped with passive suspension systems prove to be limited by the conflict between the maximal speed and the comfort of the vehicle.

A solution of this issue is presented through the employment of a semi-active central suspension, which allows the increase of the railway vehicle maximal speed and in the same time improves the railway vehicle comfort.

## ACKNOWLEDGMENTS

This work is financially supported by the UEFISCDI and is performed under the contract PN II-PCCA, no. 192/2012.

## REFERENCE

1. AHMADIAN M., YANG S., *Effect of system nonlinearities on locomotive bogie hunting stability*, *Vehicle System Dynamics*, **29**, pp. 365–384, 1998.
2. ALI ABOOD, K.H., KHAN, R.A., *Railway carriage model to study the influence of vertical secondary stiffness on ride comfort of railway carbody running on curved tracks*, *Modern Applied Science*, **5**, 2, 2011.
3. FAN, Y.T., WU, W.F., *Stability analysis of railway vehicles and its verification through field-test data*, *Journal of Chinese Institute of Engineers*, **29**, 2006.
4. GARG, V.K., DUKIPPATI, R.V., *Dynamics of Railway Vehicles Systems*, Academic Press Toronto, 1984.
5. IWNICKI, S.D., *Handbook of railway vehicle dynamics*, Taylor&Francis Group, 2006.

6. KALKER, J.J., *Wheel-rail rolling contact theory*, Wear, 1991.
7. LEE, S.Y., CHENG, Y.C., *Nonlinear analysis of hunting stability for high-speed railway vehicle trucks on curved tracks*, Journal of Vibration and Acoustics, **127**, pp. 324–332, 2005.
8. SEBESAN, I., *Dinamica vehiculelor feroviare*, Editura Tehnică, 1995.
9. SEBESAN, I., BAIASU, D., GHITA, G., *Study of the railway vehicle lateral stability using the multibody method*, INCAS Bull., **3**, pp. 89–104, 2011.
10. SEBESAN, I., BAIASU, D., GHITA, G., *Mathematical model for the study of the lateral oscillations of the railway vehicle*, UPB Sci. Bull, **74**, pp. 51–66, 2012.
11. SHABANA, A.A., *Dynamics of Multibody Systems*, Cambridge University Press, UK, 2005.
12. SHABANA, A.A., *Computational dynamics*, John Wiley & Sons Ltd, 2010.
13. WICKENS, A.H., *Fundamentals of rail vehicles dynamics*, Swets&Zeitlinger, 2003.

*Received February 11, 2014*